Biosensors and Bioelectronics 141 (2019) 111446

Contents lists available at ScienceDirect

Biosensors and Bioelectronics

journal homepage: www.elsevier.com/locate/bios

A facile homogeneous electrochemical biosensing strategy based on displacement reaction for intracellular and extracellular hydrogen peroxide detection

Fengjuan Liu[1], Limin Yang[1], Xuehan Yin, Xiaojuan Liu, Lei Ge**, Feng Li*

College of Chemistry and Pharmaceutical Sciences, Qingdao Agricultural University, Qingdao, 266109, People's Republic of China

ARTICLE INFO

Keywords:
Homogeneous electrochemical biosensor
Displacement reaction
Intracellular and extracellular hydrogen peroxide
Living cells

ABSTRACT

Traditional electrochemical hydrogen peroxide (H_2O_2) assays all indispensably require the immobilization of enzyme or nanomaterials on electrode surface. These complex electrode surface modifications are laborious and time-consuming. To overcome such limitations, we developed here a facile homogeneous electrochemical biosensor based on displacement reaction for detection of intracellular and extracellular H_2O_2 produced by living cells. Methylene blue-labeled short single-stranded DNA strand (DNA-MB) was ingeniously designed as the reporter, which was adsorbed on CeO_2 nanoparticles to result in low electrochemical signal. In the presence of H_2O_2, DNA-MB was released from CeO_2 nanoparticles, leading to the significant enhancement of current signal. Therefore, a simple homogeneous electrochemical H_2O_2 assay is successfully achieved. This strategy also displays excellent anti-interference capability and reproducibility for H_2O_2 determination. More importantly, this method was capable of conveniently realizing intracellular and extracellular H_2O_2 assay. Thus, with the excellent merits of simplicity, rapidness, good repeatability, high specific and sensitivity, the proposed strategy has great potential to be applied in exploring the roles of H_2O_2 in physiological and pathological processes.

1. Introduction

Reactive oxygen species (ROS) are important biochemical mediators in cellular physiology and pathology (Finkel, 2005; Li et al., 2016a). In particular, hydrogen peroxide (H_2O_2) is an important representative of ROS molecules in living organisms (Rhee, 2006; Weinstain et al., 2014). Emerging evidences have demonstrated that maintaining H_2O_2 concentration at normal level was critical in biological events such as cell growth and signal transduction, while disruption of its physiologic homeostasis would result in many serious diseases (Lundgren et al., 2018; Lippert et al., 2011). Meanwhile, the long lifetime of H_2O_2 makes it be able to diffuse into cellular compartments as well as extracellular environment. Once diffused out of the cell membrane, extracellular H_2O_2 impacts cell migration, cellular communications and so on. The intracellular concentration of H_2O_2 was at the level of 0.05–0.7 μM and the extracellular H_2O_2 concentration was about 10-fold higher than the intracellular level under normal conditions, while the local intracellular and extracellular concentrations of H_2O_2 will be increased under pathological conditions (Antunes and Cadenas, 2001; Boveris et al., 2002). Therefore, it is of great significance to develop a simple, sensitive and selective method to measure both intracellular and extracellular H_2O_2 concentrations, which will be favorable to explore the roles of H_2O_2 in occurrence and evolvement of diseases.

Until now, many techniques have been explored for the detection of H_2O_2, including fluorescence, chemiluminescence, and electrochemical methods, and so on (Chen et al., 2014; Quintino et al., 2005; Xu et al., 2013; Lebiga et al., 2015; Yoon et al., 2017). Among these methods, the electrochemical H_2O_2 assays have attracted much attention due to the outstanding advantages such as simple instrumentation, easy miniaturization, and convenient operation procedures (Liu et al., 2013; Shi et al., 2014; Li et al., 2014). Over the past decade, a variety of the enzyme-based methods have been developed for H_2O_2 determination (Liu et al., 2017; Chen et al., 2016; Kafi et al., 2008; Koposova et al., 2015). Nevertheless, the intrinsic shortcomings associated with enzyme-based detection methods in terms of high cost, environmental instability and denaturation inevitably limit their practical applications. Therefore, to overcome these limitations, non-enzymatic electrochemical H_2O_2 sensors have drawn particular attention. Since direct

* Corresponding author.
** Corresponding author.
E-mail address: lifeng@qau.edu.cn (F. Li).
[1] F. Liu and L. Yang contributed equally to this work.

https://doi.org/10.1016/j.bios.2019.111446
Received 10 April 2019; Received in revised form 31 May 2019; Accepted 17 June 2019
Available online 19 June 2019

detection of H_2O_2 at solid electrodes usually requires a relatively high overpotential, great efforts have been made to utilize nanomaterials as effective electrocatalysts for developing nonenzymatic electrochemical H_2O_2 sensors (Wang et al., 2013, 2015; Li et al., 2015b, 2016b; Sun et al., 2016, 2017; Bai et al., 2016; Wu et al., 2012; Ju and Chen, 2015; Dou et al., 2018). These methods have witnessed promising progresses, but some drawbacks still exist, including expensive raw materials, harsh reaction conditions and complex nanomaterials preparation processes. More importantly, these reported traditional electrochemical sensing methods for H_2O_2 assay all indispensably required the immobilization of enzyme or nanomaterials on electrode surface, which were laborious and time consuming. Meanwhile, these tedious electrode modification processes also impaired the reproducibility of the biosensors. As a consequence, it is greatly desirable to develop facile and easier-to-use immobilization-free electrochemical approaches for H_2O_2 detection.

More recently, homogeneous electrochemical biosensing strategies have been intelligently explored, which open a new way for the development of immobilization-free electrochemical sensors (Luo et al., 2008). In a typical homogeneous electrochemistry biosensor, the analyte recognition is performed in solution phase instead of on the electrode surface and the quantitative determination of analyte is performed by detecting the changes of current of electroactive substance labeled DNA to the electrode surface. Therefore, compared with conventional immobilization-based electrochemical approaches, homogeneous electroanalytical technique possesses noticeable advantages, such as avoiding the tedious and time-consuming modification processes, which effectively improves the reliability and reproducibility of homogeneous electrochemical biosensors. In virtue of these remarkable advantages, numerous homogeneous electrochemical systems have been proposed for successful detection of all sorts of targets, such as metal ions, DNA, microRNA, small biological molecules, and so on (Xuan et al., 2013, 2015; Miranda-Castro et al., 2012; Zhuang et al., 2014; Hou et al., 2015; Liu et al., 2015b; Zhang et al., 2015; Tan et al., 2015; Ge et al., 2016; Li et al., 2015a). For instance, Hsing and coworkers achieved sensitive detection of DNA and mercury ion by utilizing homogeneous electrochemical strategies (Luo et al., 2008; Xuan et al., 2015; Miranda-Castro et al., 2012). Our group also reported highly sensitive homogeneous electrochemical biosensing methods for analysis of carcinoembryonic antigen, transcription factor, microRNA and human telomerase (Hou et al., 2015; Liu et al., 2015b; Zhang et al., 2015; Ge et al., 2016; Li et al., 2015a).

Herein, inspired by the aforementioned works, we propose a simple and reliable immobilization-free electrochemical biosensor for "signal-on" detection of intracellular and extracellular H_2O_2 based on the displacement reaction. It has been reported that the CeO_2 nanoparticles (CeO_2 NPs) displayed different coordination affinities toward single-stranded DNA (ssDNA) and H_2O_2 (Gao et al., 2016; Liu et al., 2015a). The ssDNA could easily adsorb on the surface of CeO_2 NPs and thus forming the CeO_2-DNA nanocomposite. Because H_2O_2 possesses much stronger coordination effect toward CeO_2 NPs than ssDNA, the adsorbed ssDNA thus would be released from the nanocomposite in the presence of H_2O_2. In this strategy, by utilizing the diffusivity difference of ssDNA and CeO_2-DNA complex toward the negatively charged indium tin oxide (ITO) electrode, a simple immobilization-free electrochemical method for sensing of H_2O_2 was readily developed. As shown in Scheme 1, a methylene blue-labeled short ssDNA strand with 5 bases (denoted as DNA-MB) was reasonably designed and used as the reporter. After adding CeO_2 NPs into DNA-MB solution, CeO_2-DNA-MB nanocomposite was formed, which hardly be in close proximity to the negatively charged ITO electrode surface because of its low diffusivity, thus a small current signal was observed. In the presence of H_2O_2, it readily displaced the adsorbed DNA-MB from CeO_2 NPs, thus a large amount of free DNA-MB molecules were released in the solution. Due to its small size and less negative charges, free DNA-MB was able to easily access the surface of the electrode, producing much enhanced electrochemical signal. Therefore, the as-proposed homogeneous electrochemical method, with excellent merits of simplicity, rapidness and high sensitivity, was successfully applied in detecting intracellular and extracellular H_2O_2 generated by living cells. As far as we know, it is first reported homogeneous electrochemical biosensor for the analysis of H_2O_2 until now.

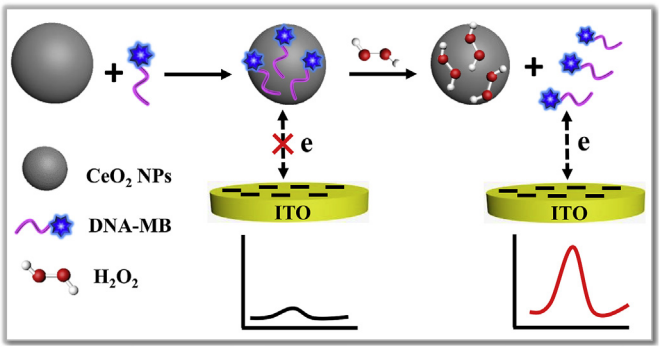

Scheme 1. Principle of the immobilization-free electrochemical strategy for H_2O_2 assay.

2. Experimental section

2.1. Reagents and materials

Cerium (III) nitrate ($Ce(NO_3)_3{\cdot}6H_2O$, 99.99%) was purchased from Shandong Xiya Chemical Industry Co. Ltd. Dopamine, ethanol, tris (hydroxymethyl)aminomethane (Tris), hydrogen peroxide (H_2O_2), hydrochloric acid (HCl), glucose, sucrose, lactose, sodium chloride (NaCl) and magnesium chloride ($MgCl_2{\cdot}6H_2O$) were purchased from Sinopharm Chemical Reagent Co., Ltd. (Shanghai, China). Ascorbic acid, uric acid, histidine, glutamate, lysine, serine, glutathione, cysteine, HRP and phorbol 12-myristate13-acetate (PMA) were obtained from Sigma-Aldrich (Shanghai, China). The human breast cancer cell line MCF-7 was purchased from Procell Life Science&Technology Co., Ltd (Wuhan, China). All reagents are of analytical grade and used without further purification. All aqueous solutions were prepared using ultrapure water obtained from a Milli-Q water purification system (Millipore Corp., Bedford, MA, USA). Methylene blue-modified oligonucleotide was synthesized and purified by Sangon Biotechnology Co., Ltd. (Shanghai, China), with the following sequence: 5′-methylene blue-AAAAA-3'.

2.2. Apparatus and instrumentation

Differential pulse voltammetric (DPV) measurements were measured on an Autolab electrochemical workstation (Metrohm, Netherlands) using a conventional three-electrode cell: an ITO working electrode, an Ag/AgCl reference electrode and a platinum wire counter electrode. Transmission electron microscopy (TEM) was carried out on a HT7700 microscope (Hitachi, Japan) operated at 100 kV. Absorption spectra were recorded on a pharmaspec UV-1700 UV-visible spectrophotometer (Shimadzu, Japan). X-ray diffraction (XRD) analysis was performed with D8 ADVANCE (Bruker AXS) X-ray diffractometer. Zeta potential was measured on dynamic light scattering on the Zetasizer Nano ZEN3690 (Malvern Instruments Ltd., Malvern, UK). The scanning electron microscopy (SEM) and elemental analysis were performed on S-4800 (Hitachi, Japan) with an accelerating voltage of 15 kV.

2.3. ITO electrode pretreatment

Before electrochemical detection, the ITO electrode was sequentially sonicated in ethanol and ultrapure water for 30 min. Then, it was

soaked in 1 mM NaOH solution for 5 h, followed by sonication in ultrapure water for 10 min. Finally, a negatively charged working electrode surface was achieved.

2.4. Synthesis of CeO_2 NPs

CeO_2 NPs were synthesized using a reported method with some modifications (Mai et al., 2005). Briefly, 5 mL of $Ce(NO_3)_3$ solution (57 mM) was added dropwise into 35 mL of NaOH solution (80 mM) under vigorous stirring. After 30 min, the obtained white slurry mixture solution was added into an autoclave and kept at 180 °C for 24 h. After that, the as-prepared nanoparticles were washed by ultrapure water and ethanol for several times, respectively, and dried at 60 °C overnight to afford CeO_2 powders.

2.5. Homogeneous electrochemical H_2O_2 assay

The H_2O_2 assay was performed in 50 μL of reaction buffer (10 mM Tris-HCl, 50 mM NaCl, pH 7.4) containing 1 μM DNA-MB, CeO_2 NPs (100 μg/mL), and H_2O_2 with various concentrations. The experiment without adding H_2O_2 was used as the control group. To investigate the selectivity of the as-proposed biosensor toward H_2O_2, glucose, sucrose, lactose, ascorbic acid, uric acid, histidine, glutamate, lysine, serine, glutathione and cysteine were examined. The measuring process was the same as described above but using these substances instead of H_2O_2.

2.6. Cell culture

The human breast cancer cell line MCF-7 was cultured in RPMI 1640 supplemented with 10% fetal bovine serum and 1% penicillin-streptomycin at 37 °C in a humidified environment containing 5% CO_2.

2.7. Detection of intracellular and extracellular H_2O_2

To detect intracellular H_2O_2, the PMA stimulated cell extracts was prepared. The non-treated MCF-7 cells were divided into three groups, each with the concentration of 5.0×10^6 cells mL^{-1} counted by a hemocytometer. The first group was not treated with PMA and used as the control group. The other two groups were treated with PMA (1 μg/mL) for 0.5 h. Subsequently, all the three groups of cells were suspended in 1 mL buffer solution (10 mM Tris-HCl, 50 mM NaCl, pH 7.4), respectively, and disrupted for 10 min using ultrasonic cell disruptor. Next, one group of PMA stimulated cell extract was incubated with HRP (300 U/mL) for 0.5 h. Then, the broken cell suspension of all three groups were centrifuged and the supernatant was collected. Finally, electrochemical measurements were carried out on the supernatant after diluted 10 times.

To further detect extracellular H_2O_2 released from living cells, the MCF-7 cells were plated on Petri dish for 24.0 h. After the cells (5×10^6) were washed three times with PBS, PMA with different concentrations in buffer solution (0.1, 0.5 and 1.0 μg/mL) were added to stimulate the cells for 0.5 h. The cells with no PMA stimulation were used as the control. Subsequently, the culture solution of all PMA treated groups were collected. Finally, electrochemical measurements were carried out on the culture solution after diluted 10 times.

3. Results and discussion

3.1. Characterization of CeO_2-DNA nanocomposite

We synthesized the CeO_2 NPs by a facile previously reported hydrothermal method (Mai et al., 2005). TEM and SEM images showed that the diameter of the as-prepared CeO_2 NPs was about 20.0 ± 2.6 nm (Fig. 1a and b). The maximum absorption of the CeO_2 NPs was observed at approximately 290 nm from the UV − vis absorption spectra (Fig. S1). Moreover, XRD spectrum (Fig. S2) indicated that the CeO_2 NPs have typical fluorite cubic structure. Then, the CeO_2–DNA nanocomposite was easily prepared through directly mixing the CeO_2 NPs and ssDNA solution, because ssDNA could adsorb on the surface of the CeO_2 NPs by the coordination effect. As shown in Fig. 1c, the Ce, O, N and P elements were obviously observed for CeO_2-DNA nanocomposite. Zeta-potential tests were also performed to investigate whether the ssDNA has been assembled on the surface of CeO_2 NPs. As illustrated in Fig. 1d, the zeta potential value of the CeO_2 NPs was +1.3 ± 0.2 and shifted to −12.5 ± 1.7 after adsorption of ssDNA. All these results demonstrated that the ssDNA has been successfully assembled on the surface of CeO_2 NPs.

3.2. Feasibility investigation of the H_2O_2 assay

Before performing the H_2O_2 assay, the feasibility of the proposed strategy was evaluated by measuring DPV signals. As shown in Fig. 2A, when the system contained only DNA-MB and CeO_2 NPs, a small peak current of about 18 nA was observed (red line) due to the weak diffusivity of CeO_2-DNA-MB nanocomposite towards the electrode. With the addition of H_2O_2 into the system, the DPV signal exhibited a significant increase (black line). This is because H_2O_2 can displace the adsorbed DNA-MB from CeO_2-DNA-MB nanocomposite, thus generating multiple free DNA-MB reporters. Due to its small size and less negative charges, DNA-MB shows much larger diffusivity than that of CeO_2-DNA-MB nanocomposite towards the negatively charged ITO electrode surface. Therefore, the generated DNA-MB was able to reach the electrode surface with much ease, resulting in big electrochemical signal. Moreover, the redox peak currents of MB also showed obvious increase in the presence of H_2O_2 (Fig. S3). Taken together, these proof-of-concept tests shows the feasibility of using DNA-functionalized CeO_2 NPs for rapid and facile detection of H_2O_2.

3.3. Optimization of experimental conditions

In order to get the best performance, some experimental parameters were carefully optimized. The initial amount of CeO_2 NPs is crucial to the analytical performance of the biosensor. If CeO_2 NPs are not enough, a high background signal will result, and excessive amount of CeO_2 NPs will affect the detection sensitivity. Thus, the impact of the CeO_2 NPs concentration on the current of DNA-MB was first evaluated. As shown in Fig. 2B, the peak currents of DNA-MB gradually reduced with increased amount of CeO_2 NPs. When the amount of CeO_2 NPs increased to 100.0 μg/mL, the DPV signal levelled off (Fig. 2C). This could be the result of the low diffusivity of CeO_2-DNA-MB nanocomposite, making it hardly be in close proximity to the negatively charged ITO electrode surface. Therefore, the peak current of DNA-MB gradually reduced with the increase of CeO_2 concentration. Moreover, the peak current of the MB molecules almost not changed by directly mixing the MB molecules and CeO_2 NPs (Fig. S4), demonstrating that the reduced current of DNA-MB definitely contributed to its adsorption on CeO_2 NPs surface. Therefore, 100.0 μg/mL was used as the optimal concentration of CeO_2 NPs in the subsequent experiments. Next, a time-course experiment was carried out to study the speed of the reaction between CeO_2 NPs and DNA-MB. The concentrations of DNA-MB and CeO_2 NPs were set as 1.0 μM and 100.0 μg/mL, respectively. It should be noted that the DPV signal sharply decreased after CeO_2 NPs mixed with DNA-MB within 2 min (Fig. S5), and then reached a plateau, indicating a fast adsorption of DNA-MB on the surface of CeO_2 NPs. Moreover, the reaction time was also investigated to guarantee the complete reaction between H_2O_2 and CeO_2-DNA-MB nanocomposite. Fig. 2D showed that the DPV peak current change ΔI_p ($\Delta I_p = I_p - I_{p,0}$, in which I_p and $I_{p,0}$ are the peak currents in the presence and absence of H_2O_2, respectively) enhanced progressively with the increase of reaction time and reached a plateau after 10 min. Therefore, 10 min was selected as the optimal reaction time and used for the following study.

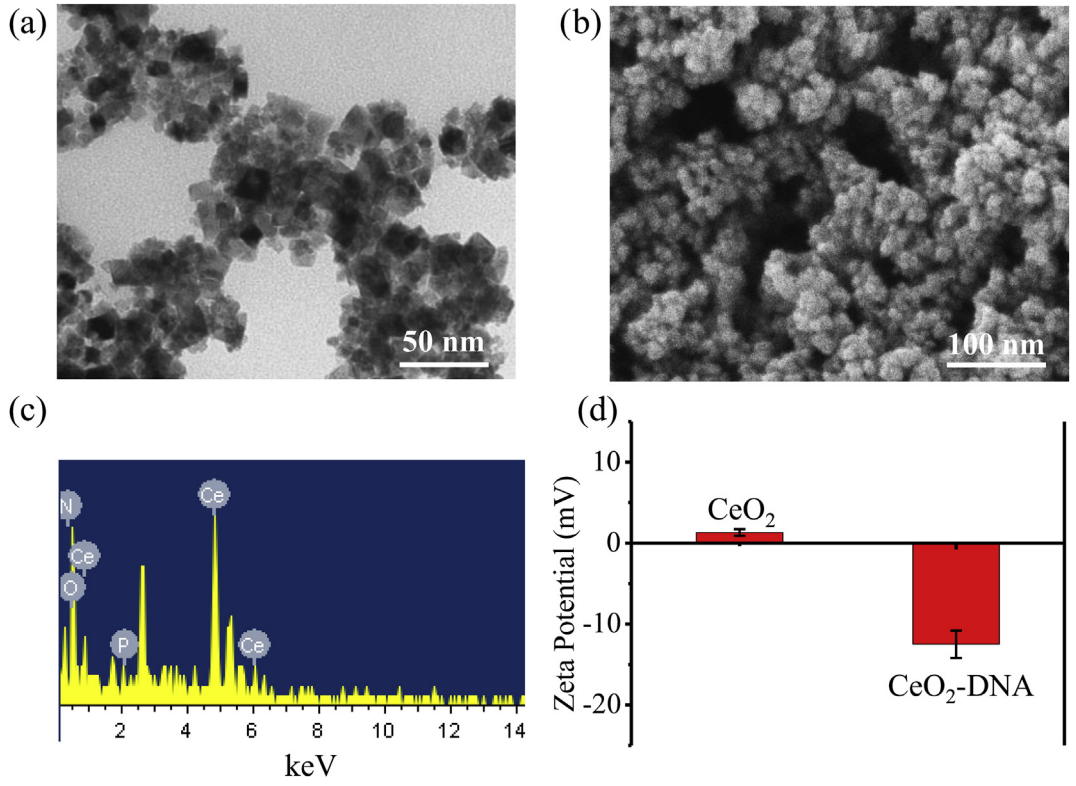

Fig. 1. Characterization of the CeO_2-DNA nanocompsite. (a) TEM and (b) SEM images of the CeO_2 NPs. (c) EDX analysis elemental composition of CeO_2-DNA nanocomposite. (d) Zeta potential of CeO_2 NPs and CeO_2-DNA nanocompsite.

3.4. Homogenous electrochemical biosensing of H_2O_2

Under the optimized experimental conditions, the performance of the developed homogeneous electrochemical biosensor toward H_2O_2 with different concentrations was investigated. Fig. 3A showed that the DPV signal gradually enhanced with the increase of the concentration of H_2O_2. The DPV peak current change ΔI_p ($\Delta I_p = I_p - I_{p,0}$, in which I_p and $I_{p,0}$ are the peak currents in the presence and absence of H_2O_2, respectively) gradually increased with the augment of H_2O_2 concentration from 0.1 to 40.0 μM (Fig. 3B). The enhanced current signals could be attributed to the fact that the increased amount of H_2O_2 caused more DNA-MB released into the solution. Compared with the CeO_2-DNA-MB nanocomposite, the DNA-MB are easier to reach the electrode surface due to the weak electrostatic repulsion, thus leading to increased current signal. A good linear relation between the ΔI_p and the concentration of H_2O_2 was clearly observed (inset of Fig. 3B). The detection limit toward H_2O_2 was estimated to be 35 nM (S/N = 3). Furthermore, to test the repeatability of the homogeneous electrochemical approach, six replicate assays in the presence of 1.0 μM and 10.0 μM H_2O_2 were performed, respectively. The results showed that the relative standard deviations (RSDs) were calculated to be 3.9% and 3.1%, respectively, demonstrating a satisfactory repeatability of the developed strategy for H_2O_2 assay. Besides the repeatability, the reproducibility of the homogeneous electrochemical approach was also investigated with six different biosensors under the same experimental conditions. The results showed that RSD was estimated to be 3.6%, indicating the proposed method possessed acceptable reproducibility. The detection performance of the as-proposed homogeneous electrochemical biosensing system was also compared with some methods reported in literature (Table S1), implying an acceptable and competitive detection sensitivity. More significantly, compared to those traditional heterogeneous electrochemical H_2O_2 assays, the as-proposed immobilization-free solution-phase electrochemical method avoids sophisticated immobilization procedures, making it cost-effective and easy to carry out.

3.5. Selectivity of H_2O_2 assay

Next, to investigate the selectivity of the developed homogeneous electrochemical biosensor for H_2O_2 detection, a few interference species, including histidine, glutamate, lysine, serine, glutathione and cysteine, glucose, sucrose, lactose, ascorbic acid and uric acid with the same concentration were examined, respectively. Significantly raised ΔI_p and peak currents were observed only in the presence of H_2O_2 (Fig. 4 and Fig. S6), whereas no noticeable increase of ΔI_p was observed in the presence of the above interference substances. These results definitely indicated that the developed homogeneous electrochemical strategy exhibited excellent selectivity for H_2O_2 over other competing substances, which could be attributed to the strong coordination effect between H_2O_2 and CeO_2 NPs. Taken together, these results demonstrated that the proposed biosensor is suitable for detecting H_2O_2 in biological samples.

3.6. Detection of intracellular and extracellular H_2O_2

Aberrant generation of intracellular and extracellular H_2O_2 is closely associated with multiple diseases. Determination of H_2O_2 variation is crucial to the understanding of its roles in physiology and pathology. Thus, we first examined the performance of the biosensor for detecting intracellular H_2O_2 by using PMA as the stimulant to elevate intracellular H_2O_2 levels (Srikun et al., 2008). MCF-7 cell was choose to the model cell line. As shown in Fig. 5A, a negligible enhancement of peak current was observed in cell lysate without PMA treatment (red line). However, an obvious enhancement of peak current was observed in PMA-stimulated cell lysate (blue line), indicating the dramatic increase of H_2O_2 concentration. To confirm that the change of current signal is indeed the response of intracellular H_2O_2, HRP (an H_2O_2 scavenger) was added into the PMA-stimulated cell lysate. Upon

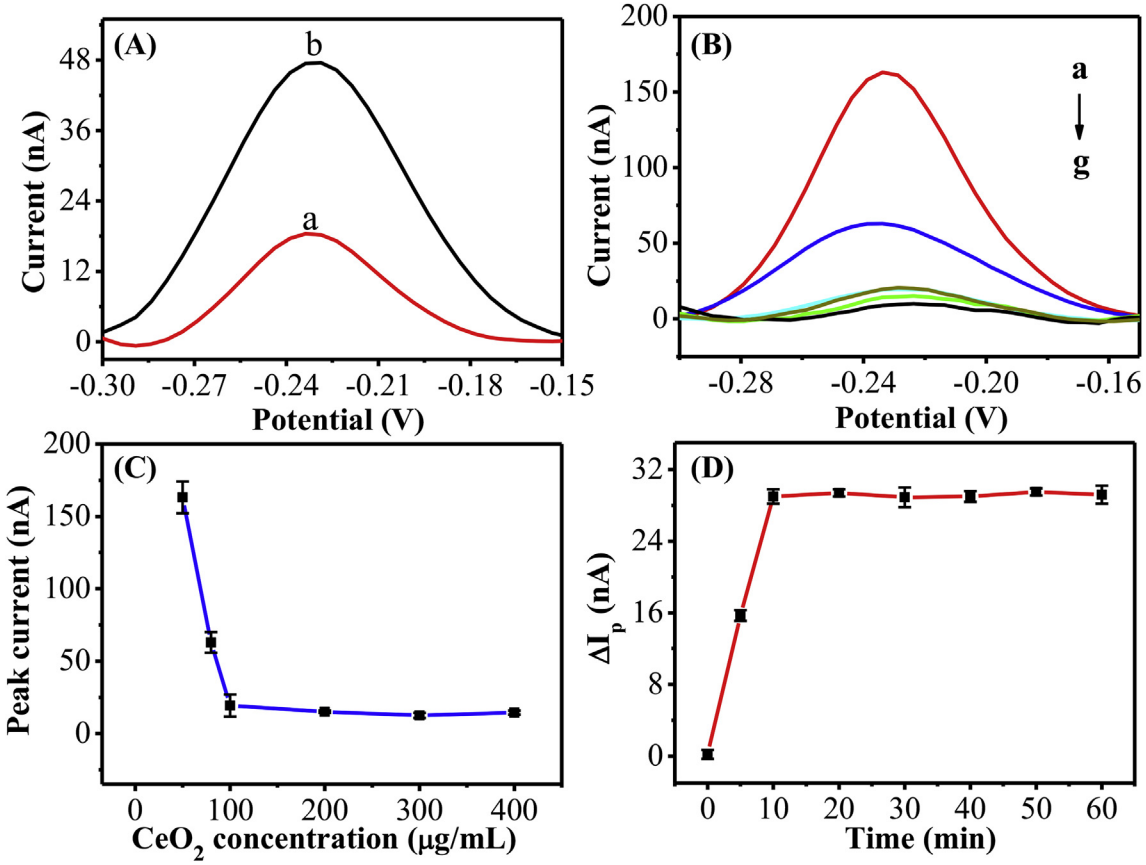

Fig. 2. (A) Differential pulse voltammograms under different conditions: (a) DNA-MB + CeO_2 NPs, (b) DNA-MB + CeO_2 NPs + H_2O_2. The concentrations of DNA-MB, H_2O_2, and CeO_2 NPs were 1.0 μM, 20.0 μM, and 100.0 μg/mL, respectively. (B) Differential pulse voltammograms of DNA-MB in the presence of CeO_2 NPs with different concentrations (from a to g: 50, 80 100, 200, 300, 400 μg/mL). (C) DPV peak currents of DNA-MB versus different concentrations of CeO_2 NPs. (D) The ΔI_p versus H_2O_2 at different times. $\Delta I_p = I_p - I_{p,0}$, in which $I_{p,0}$ is the DPV peak current in the absence of H_2O_2, and I_p is the peak current in the presence H_2O_2.

addition of HRP, the current signal of the PMA-stimulated cell lysate was noticeably reduced (green line), suggesting the successful scavenging of H_2O_2 by HRP. It is indicated that the evident the increased ΔI_p was indeed attributed to H_2O_2 produced from the PMA-stimulated cell lysate. The results of the ΔI_p value were consistent with the DPVs experiments (Fig. 5B). Next, we determined the concentration of H_2O_2 in PMA-treated cell. When the concentration of H_2O_2 in the cell lysate was higher than 1.0 μM, the lysate was properly diluted before analyzing. The H_2O_2 concentration in PMA-treated cell was calculated to about 3.8 fmol per cell. These results clearly proved that the proposed strategy could be used to evaluate the changes of the intracellular H_2O_2 level. Moreover, the RSDs were estimated to be 3.8% and 4.2% by six successive assays and six different biosensors in the presence of PMA-treated cell lysate, indicating an acceptable repeatability and reproducibility for the as-proposed method for H_2O_2 assay in real biological sample.

On the basis of the above interesting results, we next explored the feasibility of the as-proposed method for determination of extracellular

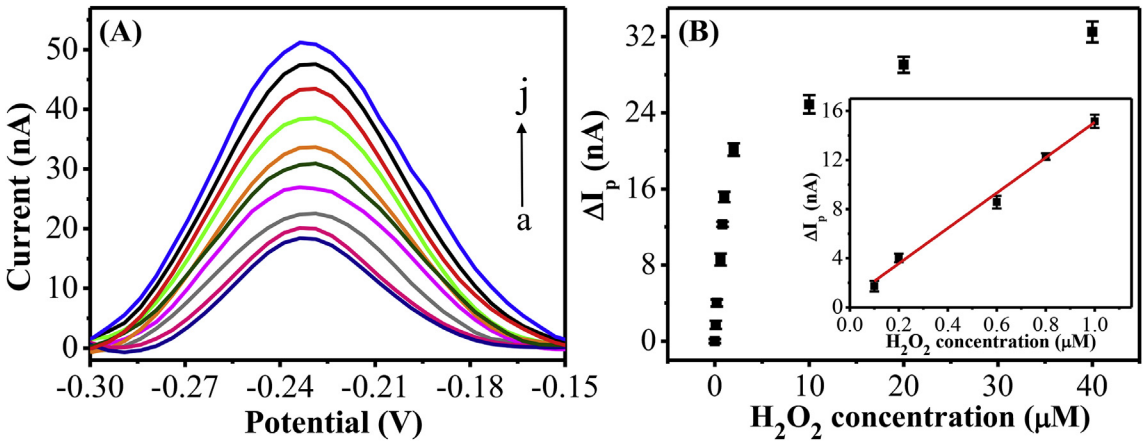

Fig. 3. (A) The DPV responses of the proposed biosensor to different concentrations of H_2O_2: (a) 0, (b) 0.1, (c) 0.2, (d) 0.6, (e) 0.8, (f) 1.0, (g) 2.0, (h) 10, (i) 20, (j) 40 μM. (B) The ΔI_p as a function of H_2O_2 concentrations. Insert shows the calibration curve of the ΔI_p versus H_2O_2 concentrations from 0.1 μM to 1.0 μM. $\Delta I_p = I_p - I_{p,0}$, in which $I_{p,0}$ is the DPV peak current in the absence of H_2O_2, and I_p is the peak current in the presence H_2O_2.

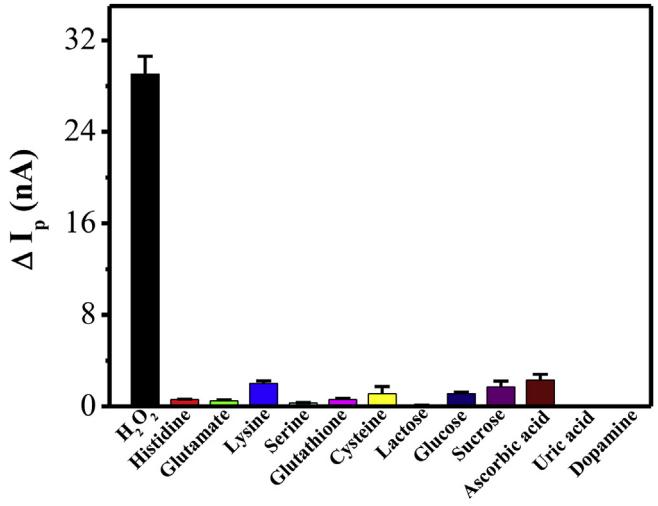

Fig. 4. Selectivity test of H_2O_2 detection toward different interference species. All interference species concentrations were tested at 20.0 μM. $\Delta I_p = I_p - I_{p,0}$, in which I_p and $I_{p,0}$ are the peak currents in the presence and absence of the interference species, respectively.

H_2O_2 released from living cells. The MCF-7 cells were incubated with different concentrations of PMA to stimulate the cells releasing H_2O_2, and MCF-7 cells without PMA simulation were used as the control group. The current signal and ΔI_p enhanced successively with the increase of PMA concentration (Fig. 5C and D), indicating that the amount of H_2O_2 released from cells exhibited a PMA dose-dependent trend. In addition, for 0.1 μg/mL, 0.5 μg/mL and 1.0 μg/mL PMA-treated cell, the amounts of H_2O_2 were estimated to be ~0.4 fmol, 1.8 fmol and 3.8 fmol generated per cell. To further confirm the selectivity of the as-proposed method for extracellular H_2O_2 released from living cells, the PMA-treated cells were further incubated with HRP. Fig. S7 showed that the ΔI_p decreased sharply after the HRP treatment. All these results evidently demonstrated that the developed homogeneous electrochemical strategy was capable of detecting intracellular and extracellular H_2O_2, and could be potentially applied in physiological and pathological researches.

4. Conclusions

In summary, a facile homogeneous electrochemical biosensor was developed for H_2O_2 assay based on displacement reaction. By making use of the diffusivity difference between DNA-MB and CeO_2-DNA-MB nanocomposite toward the negatively charged ITO electrode, and the different coordination affinities of CeO_2 NPs toward ssDNA and H_2O_2, highly sensitive and selective detection of H_2O_2 was successfully

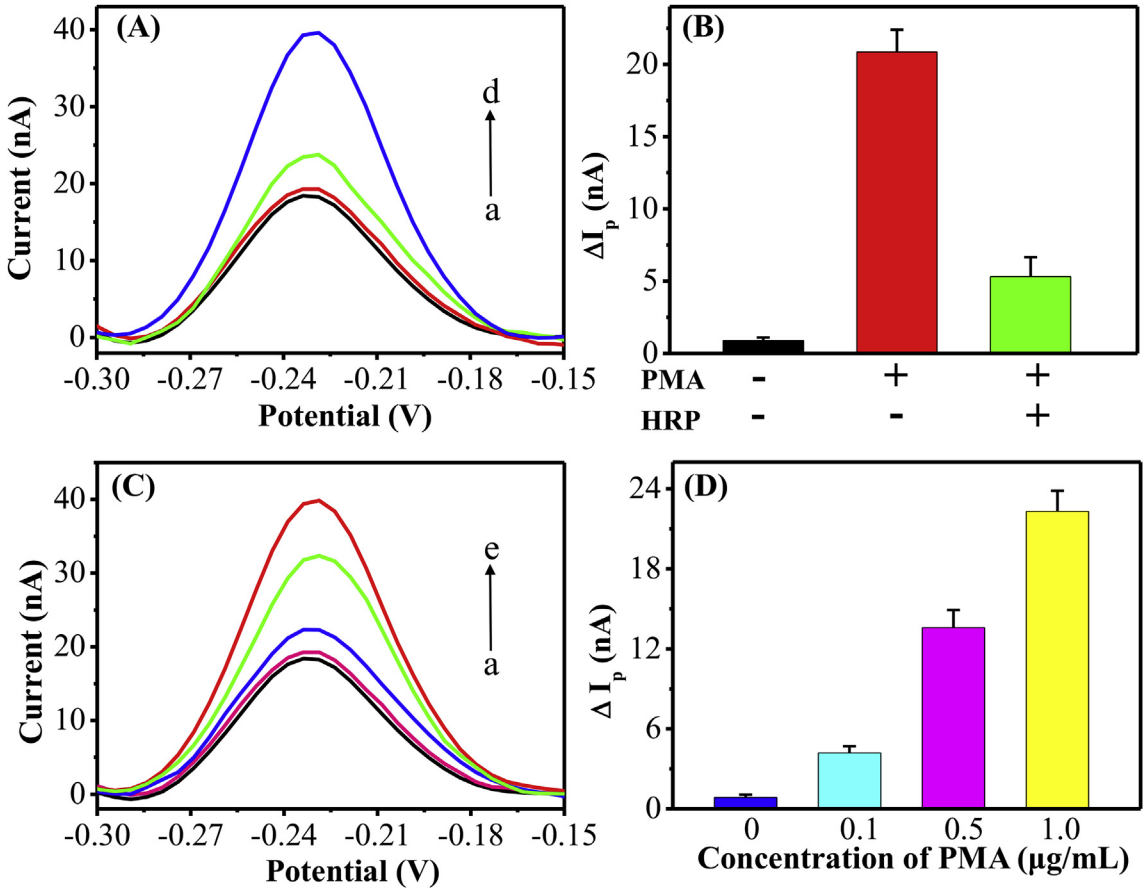

Fig. 5. (A) Differential pulse voltammograms corresponding to the analysis of intracellular H_2O_2: (a) blank, (b) the cell lysate without any treatment, (c) PMA-stimulated cell lysate + HRP, (d) PMA-stimulated cell lysate. The concentrations of PMA and HRP are 1.0 μg/mL and 300 U/mL, respectively. (B) The ΔI_p in the presence of cell lysate under different conditions. (C) Differential pulse voltammograms corresponding to the analysis of extracellular H_2O_2 released from MCF-7 cells: blank (a), culture medium without any treatment (b), culture medium collected form the cells treated with 0.1 μg/mL PMA (c), 0.5 μg/mL PMA (d) and 1.0 μg/mL PMA (e). (D) The ΔI_p in the presence of culture medium under different conditions. $\Delta I_p = I_p - I_{p,0}$, in which $I_{p,0}$ is the DPV peak current of the blank, and I_p is the DPV peak current of the detection system under different treatment. For the group without PMA and HRP, I_p was the DPV peak current of the detection system in the presence of cell lysate without any treatment. For the group without PMA, I_p was the DPV peak current of the detection system in the presence of culture medium without any treatment.

achieved. Furthermore, this strategy has been efficiently used to detect intracellular and extracellular H_2O_2. More importantly, the as-proposed homogeneous electrochemical strategy avoided the complex modification and immobilization procedures, displaying the distinctive features of simplicity, excellent specificity and good repeatability. Therefore, we anticipate that the current approach can provide new opportunities for exploring the physiological effect of H_2O_2 in various pathological conditions and diseases.

Declaration of interests

The authors declare that they have no known competing financial interests or personal relationships that could have appeared to influence the work reported in this paper.

CRediT authorship contribution statement

Fengjuan Liu: Conceptualization, Software, Supervision, Resources, Writing - review & editing. **Limin Yang:** Conceptualization, Data curation, Project administration, Software, Supervision, Resources, Writing - original draft. **Xuehan Yin:** Conceptualization, Data curation, Investigation, Methodology. **Xiaojuan Liu:** Conceptualization, Investigation, Methodology. **Lei Ge:** Conceptualization, Investigation, Methodology. **Feng Li:** Funding acquisition, Project administration, Resources.

Acknowledgments

This work was financially supported by the National Natural Science Foundation of China (Nos. 21804077, 21775083, and 21575074), and the Special Foundation for Distinguished Taishan Scholar of Shandong Province (ts201511052).

Appendix A. Supplementary data

Supplementary data to this article can be found online at https://doi.org/10.1016/j.bios.2019.111446.

References

Antunes, F., Cadenas, E., 2001. Free Radical Biol. Med. 30, 1008–1018.
Bai, Z., Li, G., Liang, J., Su, J., Zhang, Y., Chen, H., Huang, Y., Sui, W., Zhao, Y., 2016. Biosens. Bioelectron. 82, 185–194.
Boveris, A., Alvarez, S., Bustamante, J., Valdez, L., 2002. Methods Enzymol. 349, 280–287.
Chen, C., Hong, X., Xu, T., Chen, A., Lu, L., Gao, Y., 2016. Synth. Met. 212, 123–130.
Chen, S., Hai, X., Chen, X.W., Wang, J.H., 2014. Anal. Chem. 186, 6689–6694.
Dou, B., Yang, J., Yuan, R., Xiang, Y., 2018. Anal. Chem. 90, 5945–5950.
Finkel, T., 2005. Nat. Rev. Mol. Cell Biol. 6, 971–976.
Gao, W., Wei, X., Wang, X., Cui, G., Liu, Z., Tang, B., 2016. Chem. Commun. 52, 3643–3646.
Ge, L., Wang, W., Sun, X., Hou, T., Li, F., 2016. Anal. Chem. 88, 2212–2219.
Hou, T., Li, W., Liu, X., Li, F., 2015. Anal. Chem. 87, 11368–11374.
Ju, J., Chen, W., 2015. Anal. Chem. 87, 1903–1910.
Kafi, A.K.M., Wu, G., Chen, A., 2008. Biosens. Bioelectron. 24, 566–571.
Koposova, E., Shumilova, G., Ermolenko, Y., Kisner, A., Offenhäusser, A., Mourzina, Y., 2015. Sensor. Actuator. B Chem. 207, 1045–1052.
Lebiga, E., Fernandez, R.E., Beskok, A., 2015. Analyst 140, 5006–5011.
Li, P., Liu, L., Xiao, H., Zhang, W., Wang, L., Tang, B., 2016a. J. Am. Chem. Soc. 138, 2893–2896.
Li, W., Liu, X., Hou, T., Li, H., Li, F., 2015a. Biosens. Bioelectron. 70, 304–309.
Li, Z., Zhao, B., Wang, D., Wen, Y., Liu, G., Dong, H., Song, S., Fan, C., 2014. ACS Appl. Mater. Interfaces 6, 17944–17953.
Li, Z., Xin, Y., Wu, W., Fu, B., Zhang, Z., 2016b. Anal. Chem. 88, 7724–7729.
Li, Z., Xin, Y., Zhang, Z., 2015b. Anal. Chem. 87, 10491–10497.
Lippert, A.R., Van de Bittner, G.C., Chang, C.J., 2011. Acc. Chem. Res. 44, 793–804.
Liu, B., Sun, Z., Huang, P.J., Liu, J., 2015a. J. Am. Chem. Soc. 137, 1290–1295.
Liu, S., Wang, C., Zhang, C., Wang, Y., Tang, B., 2013. Anal. Chem. 85, 2282–2288.
Liu, X., Li, W., Hou, T., Dong, S., Yu, G., Li, F., 2015b. Anal. Chem. 87, 4030–4036.
Liu, Y., Liu, X., Guo, Z., Hu, Z., Xue, Z., Lu, X., 2017. Biosens. Bioelectron. 87, 101–107.
Lundgren, C.A.K., Sjöstrand, D., Biner, O., Bennett, M., Rudling, A., Johansson, A.L., Brzezinski, P., Carlsson, J., von Ballmoos, C., Högbom, M., 2018. Nat. Chem. Biol. 14, 788–793.
Luo, X., Lee, T.M.H., Hsing, I.M., 2008. Anal. Chem. 80, 7341–7346.
Mai, H.X., Sun, L.D., Zhang, Y.W., Si, R., Feng, W., Zhang, H.P., Liu, H.C., Yan, C.H., 2005. J. Phys. Chem. B 109, 24380–24385.
Miranda-Castro, R., Marchal, D., Limoges, B., Mavré, F., 2012. Chem. Commun. 48, 8772–8774.
Quintino, M.S.M., Winnischofer, H., Araki, K., Toma, H.E., Angnes, L., 2005. Analyst 130, 221–226.
Rhee, S.G., 2006. Science 312, 1882–1883.
Shi, J.J., He, T.T., Jiang, F., Abdel-Halim, E.S., Zhu, J.J., 2014. Biosens. Bioelectron. 55, 51–56.
Srikun, D., Miller, E.W., Domaille, D.W., Chang, C.J., 2008. J. Am. Chem. Soc. 130, 4596–4597.
Sun, Y., He, K., Zhang, Z., Zhou, A., Duan, H., 2016. Biosens. Bioelectron. 68, 358–364.
Sun, Y., Luo, M., Meng, X., Xiang, J., Wang, L., Ren, Q., Guo, S., 2017. Anal. Chem. 89, 3761–3767.
Tan, Y., Wei, X., Zhao, M., Qiu, B., Guo, L., Lin, Z., Yang, H.H., 2015. Anal. Chem. 87, 9204–9208.
Wang, L., Zhang, Y., Cheng, C., Liu, X., Jiang, H., Wang, X., 2015. ACS Appl. Mater. Interfaces 7, 18441–18449.
Wang, T., Zhu, H., Zhuo, J., Zhu, Z., Papakonstantinou, P., Lubarsky, G., Lin, J., Li, M., 2013. Anal. Chem. 85, 10289–10295.
Weinstain, R., Savariar, E.N., Felsen, C.N., Tsien, R.Y., 2014. J. Am. Chem. Soc. 136, 874–877.
Wu, P., Qian, Y., Du, P., Zhang, H., Cai, C., 2012. J. Mater. Chem. 22, 6402–6412.
Xu, K., Qiang, M., Gao, W., Su, R., Li, N., Gao, Y., Xie, Y., Kong, F., Tang, B., 2013. Chem. Sci. 4, 1079–1086.
Xuan, F., Fan, T.W., Hsing, I.M., 2015. ACS Nano 9, 5027–5033.
Xuan, F., Luo, X., Hsing, I.M., 2013. Anal. Chem. 85, 4586–4593.
Yoon, J., Lee, T., Jo, J., Oh, B.K., Choi, J.W., 2017. Biosens. Bioelectron. 93, 14–20.
Zhang, L., Hou, T., Li, H., Li, F., 2015. Analyst 140, 4030–4036.
Zhuang, J., Tang, D., Lai, W., Chen, G., Yang, H., 2014. Anal. Chem. 86, 8400–8407.